NUMERICAL MODELLING OF THE HYDRODYNAMIC PROFILE BLADES AND SIMULATION OF THE FLUID FLOW ACTION ON ROTOR BLADES OF THE MICRO-HYDROPOWER STATION

I. Bostan, V. Bostan, V.Dulgheru
Technical University of Moldova

1. INTRODUCTION

The river kinetic energy can be utilized with the help of water stream turbines. This type of turbines cab be easily mounted, simply operated and their maintenance costs are convenient. The water stream rate of 1m/s represents an energetic density of 500W/m^2 of the crossing section, and only one part of this energy can be extracted and converted into electrical energy. There are different conceptual solutions for the elaboration of this type of turbines. On the basis of the carried out theoretical research and undertaken computer simulations the conceptual diagram of micro-hydro-power station with pintle and blades fixed on vertical axles has been elaborated. The blades are oriented at a setting angle α , which is variable concerning the action line of the flow velocity vector $\vec{V}$ (Fig. 1).

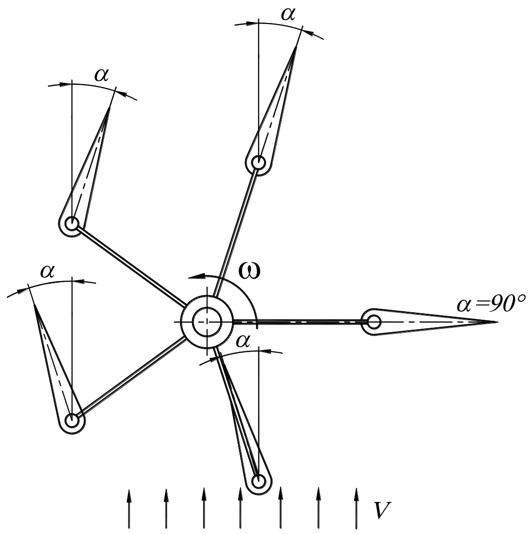

Figure 1. Conceptual diagram of the micro-hydropower station with vertical axis.

2. THE FLUID FLOW ACTION ON ROTOR BLADES

In order to carry out the numerical simulation of the interaction between the fluid flow with velocity V_∞ and the micro-hydropower station rotor blades, the „*rotor longeron – blade”* fragment is taken as basis according to Fig. 2.

Consider a symmetric profile of the blade in a fluid flow with uniform velocity $\vec{V}_\infty$ (Fig. 2.). In the fixing point O' of the symmetric blade with the boom OO' we consider two coordinate systems, namely: the $O'xy$ system with axis $O'y$ oriented in the direction of velocity vector $\vec{V}_\infty$, and axis $O'x$ normal to this direction; and the $O'x'y'$ system with axis $O'y'$ oriented along the boom direction OO', and axis $O'x'$ normal to this direction. Points A and B correspond to the trailing edge and the leading edges, respectively. The angle of attack α is the angle between the profile chord AB and $\vec{V}_\infty$, and the positioning angle φ is the angle between the boom $O'O$ and $\vec{V}_\infty$. The hydrodynamic force $\vec{F}$ has its components in directions $O'x$ and $O'y$, named lift and drag forces, respectively, given by:

$$F_L = \frac{1}{2} C_L \rho_\infty V_\infty^2 S_p, \tag{1}$$

$$F_D = \frac{1}{2} C_D \rho_\infty V_\infty^2 S_p, \tag{2}$$

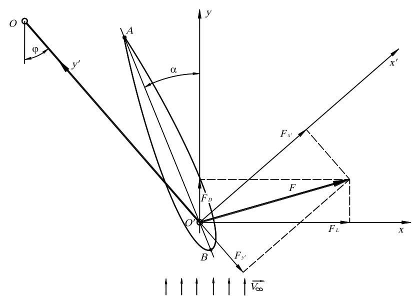

Figure 2. Rotor blade with aerodynamic profile

where ρ_∞ is the fluid density, V_∞ is the flow velocity, $S_p = ch$ (c is AB the chord length, h is the blade height) represents the lateral surface area of the blade, and C_L and C_D are the dimensionless hydrodynamic coefficients, lift and drag coefficients. Coefficients C_L and C_D are dependent on the angle of attack α, the Reynolds number Re and the aerodynamic form of the blade profile. The components of the hydrodynamic force in the coordinate system $O'x'y'$ are given by

$$\begin{aligned} F_{x'} &= -F_L \sin\varphi + F_D \cos\varphi, \\ F_{y'} &= F_L \cos\varphi + F_D \sin\varphi. \end{aligned} \tag{3}$$

The torsion moment at the rotor axis OO' developed by the blade i is

$$T_{r,i} = F_{x'} \cdot |OO'| \tag{4}$$

and the total torsion moment developed by all blades

$$T_{r\Sigma} = \sum_{i=1}^{Npal} T_{ri}\ , \tag{5}$$

where $Npal$ is the number of the rotor blades.

Since the hydrodynamic force does not have its application point in the origin of the blade axis system O', it will produce a pitching moment with respect to a reference point. Following a standard convention, the reference point is located at a ¼ of the chord distance from the leading edge B. The pitching moment, is computed by

$$M = \frac{1}{2} C_M \rho V_\infty^2 c S_p$$

where C_M represents the pitching moment coefficient.

In what follows, the profile chord is considered of unit length. Initially, consider the incompressible potential flow model. Velocity $\vec{V} = (u, v)$ at a field point $P(x, y)$ is given by

$$u(x,y) = \frac{\partial\Phi}{\partial x},\ v(x,y) = \frac{\partial\Phi}{\partial y},$$

where Φ is the flow potential obtained by superposition of the uniform velocity flow $\vec{V}_\infty = (V_\infty \cos\alpha, V_\infty \sin\alpha)$ and a distribution of sources and vortices over the profile C. Therefore,

$$\Phi = V_\infty x \cos\alpha + V_\infty y \sin\alpha + \Phi_S + \Phi_V \tag{6}$$

where Φ_S is the potential of the source distribution of strength $q(s)$ given by

$$\Phi_S = \int_C \frac{q(s)}{2\pi} \ln(r) ds\ , \tag{7}$$

and Φ_V is the potential of vortex distribution of strength $\gamma(s)$ given by

$$\Phi_V = -\int_C \frac{\gamma(s)}{2\pi} \theta ds\ . \tag{8}$$

In Eq. (7,8) s represents the distance measured along the contour C, and (r, θ) are the polar coordinates of the point $P'(x, y)$ corresponding to the distance s (Fig. 3). Consequently, the potential in the filed point $P'(x, y)$ is given by

$$\begin{aligned} \Phi(P') = {} & V_\infty x \cos\alpha + V_\infty y \sin\alpha \\ & + \int_C \frac{q(s)}{2\pi} \ln(r) ds - \int_C \frac{\gamma(s)}{2\pi} \theta ds. \end{aligned} \tag{9}$$

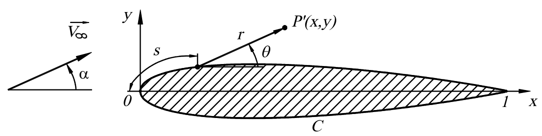

Figure 3. Notations used in the computation of the flow potential.

In order to compute Φ numerically, a collocation method is used: the boundary of the profile C is approximated with a closed polygonal line $\bigcup_{j=1}^{N} E_j$, the edges E_j having the endpoints P_j and P_{j+1} on C. The numbering of the endpoints begins from the trailing edge on the lower side in the direction of the leading edge, passing further on the upper side. Assume the vortex strength $\gamma(s)$ constant on the boundary, and the source strength $q(s) = q_j,\ j = 1,\dots,N$ constant on each boundary element E_j. Thus, Eq. (9) becomes

$$\Phi = V_\infty x\cos\alpha + V_\infty y\sin\alpha + \sum_{j=1}^{N}\int_{E_j}\left(\frac{q_j}{2\pi}\ln(r) - \frac{\gamma}{2\pi}\theta\right)ds \qquad (10)$$

with the unknowns γ and $q_j,\ j = 1,\dots,N$.

Consider the boundary element E_j with endpoints P_j and P_{j+1} (Fig. 4). The normal and tangent unit vectors of E_j are given by $n_j = (-\sin\theta_j, \cos\theta_j)$ and $\tau_j = (\cos\theta_j, \sin\theta_j)$, where

$$\sin\theta_j = \frac{y_{j+1} - y_j}{l_j},\ \cos\theta_j = \frac{x_{j+1} - x_j}{l_j}.$$

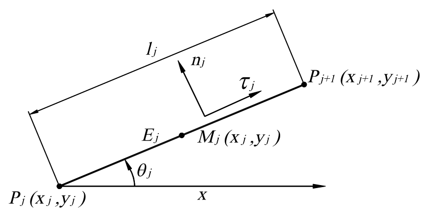

Figure 4. Boundary element E_j.

The unknowns γ and $q_j,\ j = 1,\dots,N$ are determined from the boundary condition and Kutta condition. The boundary condition $\vec{V}\cdot\vec{n} = 0$ is imposed at the collocation points $M_j\left(\bar{x}_j, \bar{y}_j\right)$, which are the middle points of the element E_j. Let $u_j = u(\bar{x}_j, \bar{y}_j)$ and $\mathrm{v}_j = v(\bar{x}_j, \bar{y}_j)$ be the velocity components at M_j. Boundary condition provides N relations

$$-u_j\sin\theta_j + v_j\cos\theta_j = 0, \quad \mathrm{j} = 1,\dots,N \qquad (11)$$

used for determining the $N+1$ unknowns γ and $q_j,\ j = 1,\dots,N$. The Kutta condition provides the final relation, namely: $\vec{V}\cdot\vec{\tau}\big|_{E_1} = \vec{V}\cdot\vec{\tau}\big|_{E_N}$, where $\vec{\tau}$ is the tangent unit vector of the boundary element. In our notations, the Kutta condition takes the form

$$u_1\cos\theta_1 + v_1\sin\theta_1 = -u_N\cos\theta_N + v_N\sin\theta_N. \qquad (12)$$

The velocity components at M_i are determined by the contributions induced by the source and vortex distributions from each element E_j

$$\begin{aligned} u_i &= V_\infty\cos\alpha + \sum_{j=1}^{N} q_j u_{ij}^s + \gamma\sum_{j=1}^{N} u_{ij}^v, \\ v_i &= V_\infty\sin\alpha + \sum_{j=1}^{N} q_j v_{ij}^s + \gamma\sum_{j=1}^{N} v_{ij}^v, \end{aligned} \qquad (13)$$

where $u_{ij}^s, v_{ij}^s, u_{ij}^v, v_{ij}^v$ are the influence coefficients computed as follows:

$$\begin{aligned} u_{ij}^s &= -\frac{1}{2\pi}\ln\left(\frac{r_{i,j+1}}{r_{ij}}\right)\cos\theta_j - \frac{\beta_{ij}}{2\pi}\sin\theta_j, \\ v_{ij}^s &= -\frac{1}{2\pi}\ln\left(\frac{r_{i,j+1}}{r_{ij}}\right)\sin\theta_j + \frac{\beta_{ij}}{2\pi}\cos\theta_j, \\ u_{ij}^v &= \frac{\beta_{ij}}{2\pi}\cos\theta_j - \frac{1}{2\pi}\ln\left(\frac{r_{i,j+1}}{r_{ij}}\right)\sin\theta_j, \\ v_{ij}^s &= \frac{\beta_{ij}}{2\pi}\sin\theta_j + \frac{1}{2\pi}\ln\left(\frac{r_{i,j+1}}{r_{ij}}\right)\cos\theta_j, \end{aligned} \qquad (14)$$

where β_{ij} is the angle between $P_j M_i$ and $P_{j+1}M_i$ for $i \neq j$, and $\beta_{ii} = \pi,\ i, j = 1,\dots,N$, and r_{ij} is the distance between M_i and P_j. Inserting Eqs. (13) and (14) in Eqs. (11) and (12) gives a linear system of $N+1$ equations with $N+1$ unknowns γ and $q_j,\ j = 1,\dots,N$. Knowing γ and $q_j,\ j = 1,\dots,N$, the tangential component of the velocity at the collocation point M_i is computed as follows (the normal component is zero):

$$u_{\tau i} = \cos(\theta_i - \alpha)V_\infty + \sum_{j=1}^{N} \frac{q_i}{2\pi}\left[\sin(\Delta_{ij})\beta_{ij} - \cos(\Delta_{ij})\ln\left(\frac{r_{i,j+1}}{r_{ij}}\right)\right] + \sum_{j=1}^{N} \frac{\gamma}{2\pi}\left[\sin(\Delta_{ij})\ln\left(\frac{r_{i,j+1}}{r_{ij}}\right) - \cos(\Delta_{ij})\beta_{ij}\right].$$

The local pressure coefficient on the discrete contour of the profile is given by

$$C_{p,j} = 1 - \left(\frac{u_{\tau j}}{V_\infty}\right)^2 .$$

The hydrodynamic force acting on E_j is given by

$$f_{xj} = C_{p,j}\left(y_{j+1} - y_j\right),$$
$$f_{yj} = C_{p,j}\left(x_{j+1} - x_j\right),$$

and the pitching moment is computed by

$$c_{m,j} = -f_{xj}\left(\frac{y_{j+1} - y_j}{2}\right) + f_{yj}\left(\frac{x_{j+1} - x_j}{2} - \frac{c}{4}\right).$$

The total force is the sum of contributions from each boundary element

$$F_x = \sum_{j=1}^{N} f_{xj}, \quad F_y = \sum_{j=1}^{N} f_{yj},$$

and the lift and moment coefficients are given by

$$C_L = -F_x \sin\alpha + F_y \cos\alpha , \qquad (15)$$

$$C_M = \sum_{j=1}^{N} c_{m,j} . \qquad (16)$$

In order to compute the drag coefficient a boundary layer analysis must be performed. The boundary layer analysis is divided into two parts: laminar and turbulent boundary layer.

The laminar boundary layer begins in the stagnation point and follows the flow along the lower or upper sides of the profile in the direction of the trailing edge. As soon as the stagnation point is determined, consider a uniform arc length partition of the upper and lower sides with the nodes being numbered toward the trailing edge.

The Thwaites model is used for the laminar boundary layer analysis. Introduce parameters: the displacement thickness δ^* given by

$$\delta^* = \int_0^\infty (1 - \frac{u}{V})dy ,$$

the thickness of impulse loss θ defined by

$$\theta = \int_0^\infty \frac{u}{V}(1 - \frac{u}{V})dy ,$$

and the thickness of energy loss θ^*

$$\theta^* = \int_0^\infty \left(1 - \left(\frac{u}{V}\right)^2\right)\frac{u}{V}dy ,$$

where V represents the velocity of the potential flow in a given point, and u is the tangential velocity in the boundary layer at this point. Consider the Von Karman integro-differential equation

$$\frac{d\theta}{dx} + \frac{\theta}{V}\left(2 + \frac{\delta^*}{\theta}\right)\frac{dV}{dx} = \frac{1}{2}C_f , \qquad (17)$$

where C_f denotes the local coefficient of the friction force on the profile surface given by

$$C_f = \frac{\tau_w}{\frac{1}{2}\rho V^2}, \text{ with } \tau_w = \mu \left.\frac{\partial u}{\partial y}\right|_{y=0} .$$

Introducing parameter $H = \frac{\delta^*}{\theta}$, Eq. (17) becomes

$$\frac{d\theta}{dx} + \frac{\theta}{V}(2 + H)\frac{dV}{dx} = \frac{1}{2}C_f . \qquad (18)$$

Multiply Eq. (17) by u and integrate to get the integral equation for the kinetic energy of the boundary layer

$$\frac{d\theta^*}{dx}+3\frac{\theta^*}{V}\frac{dV}{dx}=2C_d\,, \tag{19}$$

where the dissipation coefficient C_d is defined by

$$C_d=\frac{1}{\rho V^3}\int_0^\infty \mu\frac{\partial^2 u}{\partial y^2}dy\,.$$

Introduce the second parameter $H^*=\dfrac{\theta^*}{\theta}$ and subtract Eq. (18) from Eq. (19) to get

$$\theta\frac{dH^*}{dx}+\left(H^*\left(H-1\right)\right)\frac{\theta}{V}\frac{dV}{dx}=2C_d-H^*\frac{C_f}{2}\,. \tag{20}$$

Eqs. (18) and (20) are not sufficient for finding all the unknowns. The supplementary conditions are based on the Falkner-Skan semi-empirical relations. Denoting $\mathrm{Re}_\theta=\mathrm{Re}\cdot\theta\cdot V$, the following functional dependences are presumed

$$H^*=H^*(H)\,,\ \mathrm{Re}_\theta\frac{C_f}{2}=f_1(H)\,,\ \mathrm{Re}_\theta\frac{2C_d}{H^*}=f_2(H)\,,$$

where

$$H^*(H)=\begin{cases}1.515+0.076\dfrac{(4-H)^2}{H},\ H<4\\[2ex] 1.515+0.040\dfrac{(4-H)^2}{H},\ H\ge 4\end{cases}$$

$$f_1(H)=\begin{cases}-0.067+0.01977\dfrac{\left(7.4-H\right)^2}{H-1},\ H<7.4\\[2ex] -0.067+0.022\left(1-\dfrac{1.4}{H-6}\right),\ H\ge 7.4\end{cases}$$

$$f_2(H)=\begin{cases}0.207+0.00205\left(4-H\right)^{5.5},\ H<4\\[2ex] 0.207-0.003\dfrac{\left(4-H\right)^2}{1+0.02\left(H-4\right)^2},\ H\ge 4\end{cases}$$

Multiply Eq. (18) by Re_θ and rearrange the terms to obtain

$$\frac{V(x)}{2}\frac{d\omega}{dx}+\left(2+H\right)\omega\,W(x)=f_1(H)\,. \tag{21}$$

Multiply Eq. (20) by Re_θ/H^* and rearrange the terms to get

$$\omega\,V(x)g(H)\frac{dH}{dx}+\left(1-H\right)\omega\,W(x)=f_3(H)\,, \tag{22}$$

with the following notations $W=dV/dx$, $g(H)=d(\ln H^*)/dH$, $f_3(H)=f_2(H)-f_1(H)$. Initial values at the stagnation point are chosen such that dw/dx and dH/dx are zero.

The system of differential equations (21) and (22) is numerically solved with a backward Euler method. The method is used either until the transition from laminar to turbulent boundary layer is predicted or until the trailing edge is reached. The transition is localized by Michel's criterion

$$\mathrm{Re}_\theta>\mathrm{Re}_{\theta\max}=1.174\left(1+\frac{22.4}{\mathrm{Re}_x}\right)\left(\mathrm{Re}_x\right)^{0.46},$$

where $\mathrm{Re}_x=\mathrm{Re}\cdot V\cdot x$.

Similar to the laminar boundary layer, the Von Karman integral equation for turbulent boundary layer is considered. Computations of the turbulent boundary layer parameters are done by applying the Head's model. Let be the

$$Q(x)=\int_0^{\delta(x)}u\,dy$$

volume rate of flow through the boundary layer. Then $\delta^*=\delta-Q/V$. Introducing the flux velocity $E=dQ/dx$, we get $E=d\left(V\theta H_1\right)/dx$, where $H_1=(\delta-\delta^*)/\theta$. Head supposed that the dimensionless velocity E/V is dependent only on $H_1=H_1(H)$. Cebeci and Bradshaw considered the semi-empirical relations

$$\frac{E}{V} = 0.0306(H_1 - 3)^{-0.6169}, \qquad (23)$$

$$H_1 = \begin{cases} 3.3 + 0.8234(H - 1.1)^{-1.287}, H \le 1.6 \\ 3.3 + 1.5501(H - 0.6778)^{-3.064}, H > 1.6 \end{cases}. \qquad (24)$$

The last equation used to find the unknowns θ, H, H_1 and C_f is the Ludwieg-Tillman skin friction law

$$C_f = 0.246\left(10^{-0.678H}\right)\mathrm{Re}_\theta^{-0.268}. \qquad (25)$$

Combine the Von Karman integral equation with Eqs. (23), (24) and (25) to obtain a system of differential equations:

$$\frac{d}{dx}Y = F(x, Y), \qquad (26)$$

where $Y = (\theta, H_1)^T$ and

$$F = \begin{pmatrix} -\dfrac{\theta}{V}(2+H)\dfrac{dV}{dx} + \dfrac{1}{2}C_f \\ -H_1\left(\dfrac{1}{V}\dfrac{dV}{dx} + \dfrac{1}{\theta}\dfrac{d\theta}{dx}\right) + \dfrac{0.0306}{\theta}(H_1 - 3)^{-0.6169} \end{pmatrix}.$$

Initial values are the final values provided by the laminar boundary layer. Numerical integration of Eqs. (26) is done by a second order Runge-Kutta method. The method is applied either until the trailing edge is reached or until the separation of the turbulent layer takes place.

In order to compute the drag coefficient C_D, the Squire-Young formula is used. Given θ, H and V at trailing edge A, the drag coefficient is given by

$$C_D = \left(2\theta|_A \cdot (V|_A)^\lambda\right)_{C_{\sup}} + \left(2\theta|_A \cdot (V|_A)^\lambda\right)_{C_{\inf}} \qquad (27)$$

with $\lambda = (H|_A + 5)/2$.

3. NUMERICAL RESULTS

In what follows, we compute the hydrodynamic coefficients for a rack profile standard, and, in particular, NACA profile with chord length $c = 1.3m$. The model and numerical methods described previously are implemented in MATLAB. The coefficients corresponding to NACA0016 profile with chord length $c_{ref} = 1m$: $C_{L,ref}, C_{M,ref}$ and $C_{D,ref}$ are given by formulas (15), (16) and (27), respectively. The coefficients corresponding to the profile with chord length $1.3m$ are then obtained from relations

$$C_L = C_{L,ref} \cdot 1.3,$$
$$C_M = C_{M,ref} \cdot (1.3)^2,$$
$$C_D = C_{D,ref} \cdot 1.3.$$

Figure 5 shows the hydro-dynamic power modulus $\vec{F}$, which acts on the rotor blade together with its tangential and normal components $F_{x'}, F_{y'}$ versus the positioning angle. Figure 6 shows the moment T_{ri}

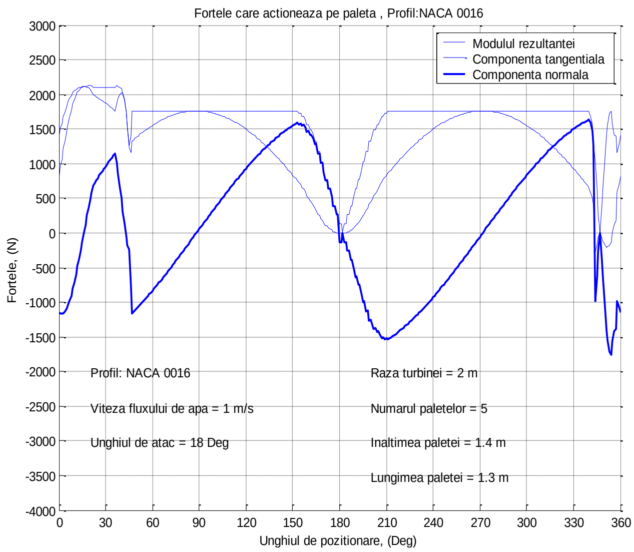

Figure 5. Hydrodynamic force acting on a blade versus the positioning angle φ.

developed by one blade versus the positioning angle, given by Eq. (4), and Fig. 7 represents the total moment of torsion $T_{r\Sigma}$ versus the positioning angle, given by Eq. (5). The moment of torsion $T_{r\Sigma}$ of rotor pin versus the positioning angle for three values of external flow velocity V_∞ is shown in Fig. 8.

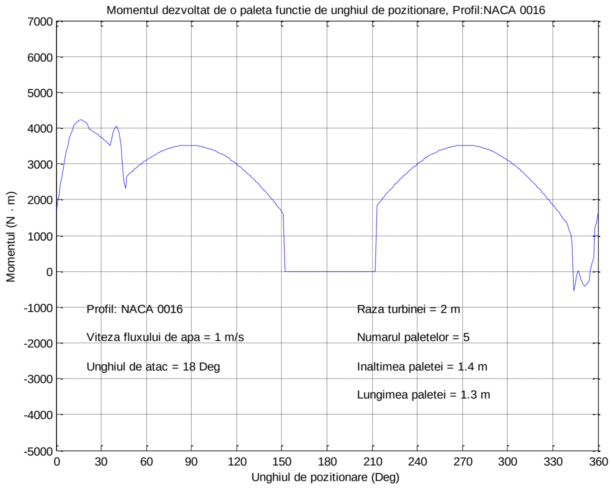

Figure 6. Moment of torsion T_{ri} developed by one blade versus the positioning angle φ .

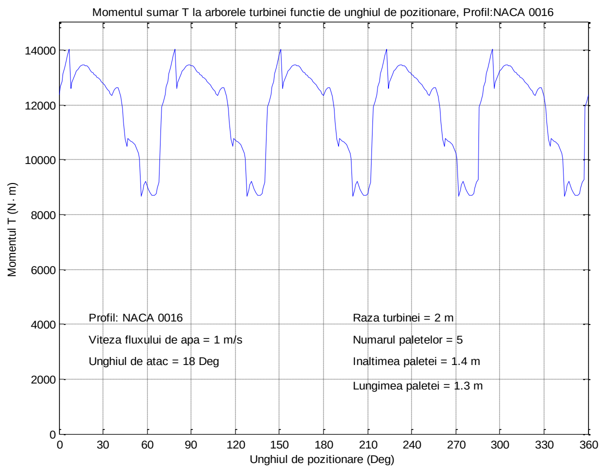

Figure 7. Total moment of torsion $T_{r\Sigma}$ developped by one blade versus the positioning angle φ .

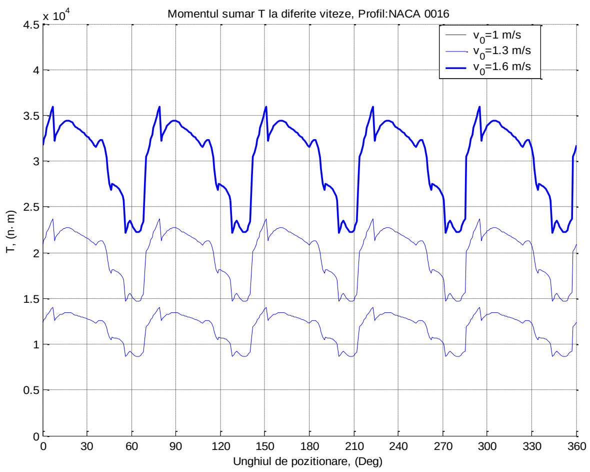

Figure 8. The moment of torsion $T_{r\Sigma}$ of rotor pin versus the positioning angle for three values of external flow velocity $V_\infty = 1m/\sec$, $1.3m/\sec$, $1.6m/\sec$.

REFERENCES

1. Drela M. *Xfoil: An Analysis and Design System for Low Reynolds Number Aerodynamics, Springer-Verlag, Lec.Notes in Eng. 54, 1989.*

2. Katz T., Plotkin A*. Low Speed Aerodynamics. Flow Wing Theory to Panel Methods. Mac-Grow Hill, 1981.*

3. Mason W.H. *Boundary Layer Analysis methods. Aerocal, 1981.*

4. Moran I. *An Introduction to Theoretical and Computational Aerodynamics, John Wiley and Sons, 1984.*

5. Bostan I., Dulgheru V., Bostan V., Sochireanu A., Trifan N. *Hydraulic turbine. Patent MD nr. 2993, 2006.*

6. Bostan I., Dulgheru V., Bostan V., Ciobanu O., Sochireanu A. *Hydraulic station. Patent MD nr. 2991, 2006.*

7. Bostan I., Dulgheru V., Sochireanu A., Bostan V., Ciobanu O., Ciobanu R. *Hydraulic station. Patent MD nr. 2992, 2006.*

Recomandat spre publicare: 09.10.2006